

Çinlar Subgrid Scale Model for Large Eddy Simulation

R. Kara^a, M. Çağlar^b

^a*Mimar Sinan Fine Arts University, Istanbul, Turkey*

^b*Koc University, Istanbul, Turkey*

Abstract

We construct a new subgrid scale (SGS) stress model for representing the small scale effects in large eddy simulation (LES) of incompressible flows. We use the covariance tensor for representing the Reynolds stress and include Clark's model for the cross stress. The Reynolds stress is obtained analytically from Çinlar random velocity field, which is based on vortex structures observed in the ocean at the subgrid scale. The validity of the model is tested with turbulent channel flow computed in OpenFOAM. It is compared with the most frequently used Smagorinsky and one-equation eddy SGS models through DNS data.

Keywords:

Stochastic flows, large eddy simulation, homogeneous turbulence, subgrid model, channel flow

1. Introduction

In fluid dynamics, the turbulent motion has chaotic and stochastic behaviour, which is modelled by the Navier-Stokes equations (NSE). On the other hand, the exact numerical or analytical solution of these equations is still open in turbulence theory. To solve NSE numerically, direct numerical simulation (DNS) is the most precise technique, which requires to include all the scales, small and large. Obviously, this procedure has a heavy computational cost. The large eddy simulation (LES), which is based on modelling the effect of the small scales on the larger scales, is an efficient numerical solution method for NSE. In LES, by applying a filter, the large scales (low

Email addresses: rukiye.kara@msgsu.edu.tr (R. Kara), mcaglar@ku.edu.tr (M. Çağlar)

frequency) are separated from the small scales (high frequency). After the filtering procedure, a nonlinear term called the subgrid scale stress (SGS) appears in LES equations. Therefore, the SGS term which remains unresolved should be modelled. It is formed by the Reynolds stress, the cross stress and the Leonard stress. The Reynolds stress consists of the fluctuations of the velocity representing the subgrid scales, the cross stress includes nonlinear interactions of the resolved and the subgrid scales, and the Leonard stress involve only the resolved velocity, which is computed numerically.

To express a physically valid closure model for the SGS stresses is the basic difficulty in LES, and many models have been proposed. Lilly [19, 20], Deardorff [9], Leonard [18] and Smagorinsky [28] are among the pioneers of the SGS models. Most commonly used subgrid stress model is Smagorinsky, an eddy viscosity SGS model proposed by Smagorinsky [28]. Moreover, assuming that the smallest resolved scales is similar to the largest unresolved scales structurally, Bardina et al. [1] developed scale similarity model. Later, a dynamic eddy viscosity model, in which the eddy viscosity coefficient is computed dynamically, is introduced by Germano, Piomelli, Moin and Cabot [12]. See also [25] for an account of various related models. Different from the above models, Misra and Pullin [22] developed a subgrid model based on stretched vortices where the orientation of the vortices is determined by the resolved scales and randomized parameters. They have taken the Reynolds stress as proportional to the energy spectrum that is expressed in terms of the vortices.

Our aim is to derive a new subgrid stress model using Çinlar random velocity field, which is also based on vortex structures [7]. Its theory has been studied extensively as a model for small to medium scale turbulent flow, see e.g. [3, 4, 5, 6]. We have recently shown that the velocity field can capture the second order properties of the subgrid scale with its energy spectrum in [16] as a plausible turbulence model. Çinlar velocity spectrum which is based on the truncated Gamma distribution indicates a good match with the spectrum estimated from real data, and it is similar to the widely used form of energy spectrum for small scales. Our initial attempts for modelling Reynolds stress have appeared in [15] where we proposed to model the energy spectrum like Misra and Pullin [22], but relying on Çinlar random velocity field as a physically valid model for the subgrid scale velocity involving vortex structures.

In this paper, we refine and develop the ideas of [15] for modelling Reynolds stress directly from the covariance tensor of Çinlar velocity field, which is

available in closed form, rather than the energy spectrum which would require more computations. Indeed, we have the analytical expression

$$\frac{\lambda}{2c} \mathbb{E}(a^2) \mathbb{E}(b^2) \int_{\mathbb{R}^2} dz \frac{v_i(z)v_j(z)}{|z|^{2\gamma}}$$

for the covariance tensor, where $\gamma > 0$ is a constant, λ , c are parameters denoting the arrival rate per unit time-unit space and the decay rate of an eddy, respectively, a is the random amplitude and b is the random radius of an eddy, and v is a standardized eddy over \mathbb{R}^2 that other eddies are obtained by randomization. The covariance at space and time lag $(0,0)$ is used as an approximation for the Reynolds stress. Then, the parameters λ , c , and the parameters originating from the probability distributions of a and b are modelled as functions of the resolved strain rate to approximate the Reynolds stress part of the SGS stress tensor. As a result, we obtain by physical and dimensional considerations an approximation of the Reynolds stress as

$$R_{ij} \equiv \delta_{ij} \frac{3\pi}{64} \frac{C_3^2 C_4}{C_1} \bar{u}^2 \bar{\Delta}^2 e^{-2C_1|\bar{S}|} f(C_2 \bar{\Delta}/(|\bar{S}|\bar{u}), C_3)$$

where C_1, \dots, C_4 are positive constants, f is an explicit function, $|\bar{S}|$ is the magnitude of the resolved strain rate, \bar{u} is the resolved velocity in LES obtained after filtering the Navier-Stokes equations, and $\bar{\Delta}$ is the grid size.

By extensive numerical computations, we compare Çinlar SGS model based on its particular Reynolds stress with two widely used SGS models, namely, Smagorinsky and one equation for Reynolds numbers 395, 590 and 950. These benchmark models are available in OpenFOAM, which is open source software for computational fluid dynamics [30]. We perform LES of fully developed incompressible turbulent channel flow in OpenFOAM. Although related, our model cannot be considered as an eddy viscosity model where only the viscosity parameter would be modelled. In our case, there is a more physical velocity model based on vortices, and the resultant model includes the parameters which are modelled with the strain rate. As a result of the computational comparison, our model is shown to provide better approximation of the fluctuations in the viscous range than the benchmark models. Besides, it is numerically efficient with less computational cost.

The paper is organized as follows. In Section 2, a brief introduction is given about LES and the benchmark SGS models. In Section 3, Çinlar velocity field is reviewed. In Section 4, Reynolds stress is modelled using

linear velocity field. Numerical results for turbulent channel flow are given in Section 5. Finally, Section 6 concludes the paper.

2. LES and SGS Models

2.1. Large Eddy Simulation

Large eddy simulation is a numerical simulation technique for turbulent flows, where the effect of small scales is modelled. LES is based on decomposing flow variables into the resolved (filtered) and the unresolved subgrid scale terms. The velocity field can be decomposed as

$$u(x) = \bar{u}(x) + u'(x)$$

where

$$\bar{u}(x) = \int_{-\infty}^{\infty} u(\xi)G(x - \xi)d^3\xi$$

is the filtered velocity field in space and G is the filter function that determines the size and structure of the small scales.

If the filtering operation is applied to Navier-Stokes equations for incompressible flows, the filtered Navier-Stokes equations are obtained as

$$\begin{aligned} \frac{\partial \bar{u}_i}{\partial x_i} &= 0 \\ \frac{\partial \bar{u}_i}{\partial t} + \frac{\partial(\bar{u}_i \bar{u}_j)}{\partial x_j} &= -\frac{\partial \bar{p}}{\partial x_i} + \nu \frac{\partial}{\partial x_j} \left(\frac{\partial \bar{u}_i}{\partial x_j} + \frac{\partial \bar{u}_j}{\partial x_i} \right) - \frac{\partial \tau_{ij}}{\partial x_j} \end{aligned} \quad (1)$$

where $\tau_{ij} = \overline{u_i u_j} - \bar{u}_i \bar{u}_j$ is subgrid scale tensor and it must be modelled to represent the effect of small scales.

Leonard [18] decomposed subgrid stress tensor as

$$\tau_{ij} = \overline{u_i u_j} - \bar{u}_i \bar{u}_j = L_{ij} + C_{ij} + R_{ij}$$

and provided physical interpretations for each term. $L_{ij} = \overline{u_i u_j} - \bar{u}_i \bar{u}_j$, the so-called Leonard tensor, represents interactions among large scales and can be computed explicitly. $R_{ij} = \overline{u'_i u'_j}$, the Reynolds stress term, represents interactions among the small scales, and $C_{ij} = \overline{u_i u'_j} + \overline{u'_j u_i}$, the cross term, represents cross-scale interactions between the resolved and unresolved scales. Modelling the non-linear term τ_{ij} is the aim of subgrid scale (SGS) models.

2.2. Subgrid Scale Models

The SGS turbulence models usually use the eddy viscosity idea focusing on energy dissipation at subgrid scale based on Boussinesq's theory, which states that the subgrid stress tensor is proportional to the resolved strain rate. Therefore, the deviatoric part of SGS stress tensor is modelled as

$$\tau_{ij}^d := \tau_{ij} - \frac{1}{3}\tau_{kk}\delta_{ij} = -2\nu_t\bar{S}_{ij}$$

where

$$\bar{S}_{ij} = \frac{1}{2} \left(\frac{\partial \bar{u}_i}{\partial x_j} + \frac{\partial \bar{u}_j}{\partial x_i} \right) \quad (2)$$

is the resolved strain rate tensor, and ν_t is the eddy viscosity. In LES, the term $\frac{1}{3}\tau_{kk}\delta_{ij}$ is embedded in the pressure term as $P = \bar{p} + \frac{1}{3}\tau_{kk}\delta_{ij}$ in (1), and only the deviatoric part τ_{ij}^d of the SGS stress tensor τ_{ij} is modelled.

Our SGS model, which is based on Çınlar velocity field for subgrid scale, also exploits the approximation of viscous effects with the resolved strain tensor. Therefore, Smagorinsky and one equation models are used as benchmark for comparison in the present work. Both are conveniently available in OpenFOAM, which is the open source software used in our computations, and are classified under eddy viscosity models.

The most common SGS model is Smagorinsky model [28]. The eddy viscosity is modelled by using the magnitude of strain rate tensor and the characteristic length scale. Characteristic length scale can be taken as proportional to the filter width with Smagorinsky constant denoted by C_S . Consequently, the eddy viscosity is given by

$$\nu_t = (C_s\bar{\Delta})^2|\bar{S}| \quad (3)$$

where

$$|\bar{S}|^2 = 2\bar{S}_{ij}\bar{S}_{ij}$$

is the magnitude of the strain rate tensor, $\bar{\Delta}$ is the grid size.

Another popular eddy-viscosity model of similar form to Smagorinsky closure relates ν_t to the subgrid scale turbulence kinetic energy of the flow k^{sgs} as [10]

$$\nu_t = C_v\bar{\Delta}\sqrt{k^{sgs}}$$

where C_v is a model constant. The turbulence kinetic energy based approach known as one equation model requires solving an extra equation for the

subgrid scale kinetic energy. The transport equation for k^{sgs} is given by [27, 13, 17]:

$$\frac{\partial k^{sgs}}{\partial t} + \frac{\partial}{\partial x_i}(\bar{u}_i k^{sgs}) = -\tau_{ij} \frac{\partial \bar{u}_i}{\partial x_j} - C_v \frac{(k^{sgs})^{3/2}}{\Delta} + \frac{\partial}{\partial x_i} \left(\nu_t \frac{\partial k^{sgs}}{\partial x_i} \right).$$

3. Subgrid Velocity Field

We consider Çinlar velocity field, which has been motivated by subgrid scale observations and shown to represent its statistical properties very well [5, 6]. Let v be a deterministic velocity field on \mathbb{R}^2 called the basic eddy, and let $Q = \mathbb{R}^2 \times \mathbb{R} \times (0, \infty)$ be the set of types of eddies. Eddies of different sizes and amplitudes for $q \in Q$, $x \in \mathbb{R}^2$ are obtained by

$$v_q(x) = a v \left(\frac{x - z}{b} \right), \quad q = (z, a, b)$$

where q represents the type of an eddy and includes its center z in space, its amplitude a as well as its radius b . Let N be a Poisson random measure on the Borel sets of $\mathbb{R} \times Q$ with mean measure

$$\mu(dt, dq) \equiv \mu(dt, dz, da, db) = \lambda dt dz \alpha(da) \beta(db)$$

where λ is the arrival rate per unit time-unit space, and α and β are probability distributions for the amplitudes and radii of eddies, respectively. The arrival time t of an eddy, its center z , amplitude a and radius b are all randomized with N . By the superposition of these eddies decaying exponentially in time with rate c_q , which depends on the type q of an eddy, the generalized form of Çinlar velocity field is constructed as

$$u'(x, t) = \int_{-\infty}^t \int_Q N(ds, dz, da, db) e^{-c_q(t-s)} a v \left(\frac{x - z}{b} \right) \quad (4)$$

where $x \in \mathbb{R}^2$, $t \in \mathbb{R}$, and the notation u' is used to indicate that we aim to model the subgrid scales with (4). The decay parameter is explicitly given by

$$c_q(x) = c \left| \frac{x - z}{b} \right|^{2\gamma}$$

for $q = (z, a, b)$, where $c > 0$ and $\gamma > 0$ [6].

The construction of Çinlar velocity field is motivated from vortex development and decay observed in the ocean [26]. Therefore, we consider an incompressible and isotropic flow in \mathbb{R}^2 by taking the basic eddy $v = (v_1, v_2)$ as a rotation around 0 with magnitude $m(r)$ at distance r from 0, where $m : \mathbb{R} \rightarrow \mathbb{R}_+$ is continuous and has support $[0, 1]$. In particular, $m(r) = (1 - \cos 2\pi r)/2$, $0 \leq r \leq 1$, and $m(r) = 0$ otherwise. The specific expressions for v are

$$v_1(x) = -\frac{x_2}{r}m(r), \quad v_2(x) = \frac{x_1}{r}m(r) \quad (5)$$

where $x = (x_1, x_2)$ and $r = |x| \in [0, 1]$.

The covariance tensor of the velocity field can be computed analytically as

$$R^{ij}(x, t) = \frac{\lambda}{c} \int_{\mathbb{R}^2} dz \int_{\mathbb{R}} \alpha(da) a^2 \int_{\mathbb{R}_+} \beta(db) \frac{b^2 \exp(-c|z|^{2\gamma}|t|)}{|z|^{2\gamma} + |z + \frac{x}{b}|^{2\gamma}} \cdot v_i(z) v_j\left(z + \frac{x}{b}\right) \quad (6)$$

for $x \in \mathbb{R}^2$ and $t \in \mathbb{R}$, where the time integral has already been taken. We will consider only small scale eddies up to some cutoff B . Therefore, the distribution β of b is chosen as a right-truncated Gamma distribution given by

$$\beta(db) = \frac{b^{\theta-1} \exp(-b/\zeta)}{\Gamma_{B/\zeta}(\theta) \zeta^\theta} db, \quad 0 < b < B \quad (7)$$

where $\theta > 0$ and $\zeta > 0$ are the shape and scale parameters, respectively, and $\Gamma_{B/\zeta}(\theta)$ is the incomplete Gamma function with parameter θ and integration bounds from 0 to B/ζ . The energy spectrum has been obtained from the Fourier transform of R with truncated Gamma distribution and studied in [16] for further validating Çinlar velocity as a plausible turbulence model.

4. Modelling Reynolds Stress

Modelling the subgrid stress tensor τ_{ij} is the key step of LES. As a term in the filtered Navier-Stokes equation, τ_{ij} reflects the effect of small scales on large scales. Recall that it is decomposed as

$$\tau_{ij} = L_{ij} + C_{ij} + R_{ij}.$$

In this section, we explain how the Reynolds stress R_{ij} is obtained and modelled. For the cross stress C_{ij} , we use Clark's cross stress model. Clark [8] has modelled cross stress using Taylor series expansion as

$$\overline{u_i u'_j} = \frac{\bar{\Delta}^2}{24} \bar{u}_i \frac{\partial^2 \bar{u}_j}{\partial x_k^2} + O(\bar{\Delta}^4) \quad (8)$$

in terms of the resolved scales. On the other hand, Leonard stress L_{ij} does not need to be modelled as it depends only on the resolved velocity field.

4.1. Reynolds Stress from Subgrid Velocity

Homogeneity and isotropy properties of turbulence indicate that the statistical properties of fluctuations u' are independent of the position and orientation. In addition, if the statistical properties do not depend on time, the random field is called stationary. So, the covariance tensor in space and time is given by

$$R^{ij}(x, t) := \mathbb{E}[u'_i(r, s)u'_j(r + x, s + t)]$$

for two-point velocity. Clearly, $R^{ij}(x, t)$ does not depend on the point r in space and the time s for homogeneous and stationary turbulence. The covariance function of Çinlar velocity field is computed as

$$R^{ij}(x, t) = \frac{\lambda}{c} \int_{\mathbb{R}} \alpha(da) a^2 \int_{\mathbb{R}^2} dz \exp(-c|z|^{2\gamma}|t|) \cdot \int_{\mathbb{R}^+} db \frac{b^{\theta-1} \exp(-b/\eta)}{\Gamma(\theta)\eta^\theta} \frac{v_i(z)v_j(z + \frac{x}{b})}{|z|^{2\gamma} + |z + \frac{x}{b}|^{2\gamma}}$$

Reynolds stress represents the interaction of small scales. In Reynolds averaged Navier-Stokes equation, Reynolds stress is defined as a time average. Because time averages converge to statistical averages by stationarity, and ergodicity when applicable, Reynolds stress is modelled as the covariance of the subgrid velocity field.

A subgrid velocity field is used to represent only small scales by definition, and hence, its covariance function corresponds to the interaction of only small scales. This is matched with the literal definition of Reynolds stress. The covariance at space and time lag (0,0) is used as an approximation for the Reynolds stress R_{ij} by

$$R^{ij}(0, 0) = \mathbb{E}[u'_i(r, s)u'_j(r, s)] \sim \overline{u'_i u'_j} = R_{ij}$$

For Çinlar velocity field, we get

$$\begin{aligned}
R_{ij} \equiv R^{ij}(0, 0) &= \frac{\lambda}{2c} \int_{\mathbb{R}} \alpha(da) a^2 \int_{\mathbb{R}^2} dz \int_{\mathbb{R}^+} \beta(db) \frac{b^2}{|z|^{2\gamma}} v_i(z) v_j(z) \\
&= \frac{\lambda}{2c} \mathbb{E}(a^2) \mathbb{E}(b^2) \int_{\mathbb{R}^2} dz \frac{v_i(z) v_j(z)}{|z|^{2\gamma}}
\end{aligned} \tag{9}$$

Substituting the basic vortex (5) in (9), we obtain the Reynolds stress as

$$R_{ij} \equiv \delta_{ij} \frac{\lambda}{c} \mathbb{E}(a^2) \mathbb{E}(b^2) \frac{3\pi}{16} \tag{10}$$

where we have taken $\gamma = 1/2$ for simplifying the result. The Reynolds stress R_{ij} will be parameterized as described below.

4.2. Modelling the Parameters of Reynolds Stress

Our aim is to represent Reynolds stress, which captures the fluctuations of the subgrid scale velocity, in terms of the resolved velocity field. The generation of small-scale fluctuations is due to the nonlinear term in the equation of motion. However, the viscous terms prevent the generation of infinitely small scales of motion by dissipating small-scale energy into heat and smoothing out the velocity fluctuations [29]. For flows with high Reynolds number, the turbulent kinetic energy, that is generated at large scales, cascades to smaller scales and then dissipates in the viscous range. On the other hand, the viscous stress depends linearly on the strain rate [24]. Therefore, the dissipation rate is directly proportional to the strain rate, which is expected to increase with the wave number.

The strain rate causes the deformation of eddies shape and local dissipation [11]. The fluid elements are extended or contracted in the straining motion. We describe a representation for each parameter appearing in the Reynolds stress (10) using these properties of the strain rate. Depending on the meaning of a parameter, we refer to viscosity, the dissipation rate, and the strain rate, interchangeably, as they are proportional to each other. Our analysis is clearly inspired by eddy viscosity models, in which the deviatoric part of the subgrid scale stress is modelled as a linear function of the strain rate tensor. However, (10) and representation of its parameters involve the aspects of vortex formation and decay as well.

Decay rate c

The eddy viscosity causes the energy dissipation. In the original Çinlar velocity field model \tilde{u} [7], small eddies are dissipated by decay rate c , due to the following equation

$$d\tilde{u}(x, t) = -c \tilde{u}(x, t)dt + \int_Q N(dt, dq).$$

that \tilde{u} satisfies. This equation does not hold with the generalized form c_q , but we use the above equation to capture the essence of the decay rate. Therefore, the parameter c is approached as eddy viscosity, or the dissipation rate. The eddy viscosity ν_t modelled by Smagorinsky [28] is proportional to the filter width and the magnitude of the strain rate. Similarly, the dissipation rate is directly proportional to the strain rate. Therefore, we set

$$c \equiv C_1 |\bar{S}|$$

where

$$|\bar{S}| = 2(\bar{S}_{ij}\bar{S}_{ij})^{1/2}$$

and $C_1 > 0$ is a constant.

Shape parameter θ and scale parameter ζ

In incompressible flows, the strain rate affects the shape of eddies and leads to their splitting into two or more smaller ones [29, pg.260]. Therefore, we also take the radius b as inversely proportional to $|\bar{S}|$. The expected value of radius b is calculated using right truncated Gamma distribution. We get

$$\mathbb{E}(b^2) = -\frac{B^\theta e^{-B/\zeta}}{\zeta^{\theta-2}\Gamma_{B/\zeta}(\theta)}(B/\zeta + \theta + 1) + \theta(\theta + 1)\zeta^2, \quad 0 < b < B$$

The shape parameter θ is unit-less and the unit of the scale parameter is characteristic length scale L . While $|\bar{S}|$ increases, smaller eddies emerge. Strain rate $|\bar{S}|$ affects directly the shape parameter θ , so we can model $\theta \propto 1/|\bar{S}|T$, where T indicates the characteristic time and it can be taken as $T = \bar{\Delta}/\bar{u}$. That is, θ is modelled by

$$\theta \equiv C_2 \frac{\bar{\Delta}}{|\bar{S}|\bar{u}}$$

where $C_2 > 0$ is a model constant. Also the change of scale parameter ζ only affects the range of the radius distribution, which is proportional to ζ . This linear relationship between ζ and B can be written as $\zeta \equiv C_3 B$, where $C_3 > 0$ is a constant.

Arrival rate λ

The arrival rate λ is defined as number of eddies per unit area and time. Therefore, its dimension is $1/(TL^2)$. Due to occurrence of new small eddies as a result of the strain rate, the number of eddies per unit area and time in subgrid scale increases. This implies that λ is proportional to the strain rate. Using this information and dimension analysis, we get

$$\lambda \equiv C_4 \frac{|\bar{S}|}{\bar{\Delta}^2}$$

where $C_4 > 0$ is a model constant.

Expectation of a^2

Lundgren and Burgers [2, 21] assume that the radial velocity decreases linearly with the strain rate. However, in Çinlar velocity field (4), the radial velocity magnitude, which is described by a , decreases exponentially in time. We note this by the term

$$e^{-c_q(t-s)} a v_q(x).$$

Then, the radial velocity simply becomes $e^{-c}a$ after a unit time increment $t - s \equiv 1$, from the initial magnitude a of the arriving vortex v_q . Clearly, the square of the initial magnitude a decays with the rate e^{-2c} .

At each time step of LES, we assume that the initial velocity at the beginning of this time step, namely \bar{u} acts as a proxy to an average value for the magnitude a of each arriving vortex in the subgrid scale. Then, since the magnitude would decay with the rate e^{-c} as explained above, we can model its square $\mathbb{E}(a^2)$ as $\bar{u}^2 e^{-2c}$ for a unit time of decay. Therefore, the second moment of a is taken to be proportional to the exponential of the strain rate as

$$E(a^2) \equiv \bar{u}^2 e^{-2C_1|\bar{S}|}$$

in view of the approximation $c \equiv C_1|\bar{S}|$.

Using our arguments above, we get the model for the Reynolds stress as

$$R_{ij} \equiv \delta_{ij} \frac{3\pi}{64} \frac{C_3^2 C_4}{C_1} \bar{u}^2 \bar{\Delta}^2 e^{-2C_1|\bar{S}|} \left[\theta(\theta + 1) - \frac{C_3^{-\theta}}{e^{1/C_3} \Gamma_{1/C_3}(\theta)} \left(\frac{1}{C_3} + \theta + 1 \right) \right] \quad (11)$$

where the radius of the largest eddy in dissipation range B is taken to be equal to half of the grid size as $\bar{\Delta}/2$, and $C_2 \bar{\Delta}/(|\bar{S}| \bar{u})$ will be used for θ as discussed above.

5. Numerical Results and Comparison

In this section, the channel flow results of the LES simulation with three different SGS models, namely, Çınlar, Smagorinsky and one equation eddy, are compared with the DNS performed by Moser et al. [23] for friction Reynolds numbers of 395 and 590, and by Hoyas and Jimenez [14] for a friction Reynolds number of 950. The friction Reynolds number is defined as $Re_\tau = u_\tau \delta / \nu$ where $u_\tau = \tau_\omega / \rho$ is the friction velocity, τ_ω is the wall shear stress and δ is the channel half height. Fully developed channel flow has been studied extensively to increase the understanding of the mechanics of wall-bounded turbulent flows and it is a baseline for validation of a turbulence model. The periodic boundary condition in the streamwise and spanwise directions, and no-slip boundary condition on the wall have been applied.

LES is performed by using the OpenFOAM CFD Toolbox [30]. A finite-volume based method is used for numerical calculations in OpenFOAM LES solver. The PIMPLE algorithm is used for the pressure-velocity coupling. For the pressure, the Poisson equation is solved using an algebraic multi-grid (AMG) solver. When the scaled residual becomes less than 10^{-6} , the algebraic equation is considered to have converged. Using adjustable time step, the time step has been modified dynamically to guarantee a constant Courant number of 0.2. The computational mesh are $128 \times 98 \times 128$ for $Re_\tau = 395, 590$ and $128 \times 128 \times 128$ for $Re_\tau = 950$. The box size is $2\pi\delta \times 2\delta \times \pi\delta$ for the streamwise, wall-normal and spanwise directions, respectively.

The numerical results are depicted through graphs of the time and space averaged quantities normalized by the friction velocity u_τ :

- the mean streamwise velocity $\langle \bar{u} / u_\tau \rangle$,
- the x, y component of the Reynolds stress $\langle u'v' \rangle / u_\tau^2$,
- the mean squared (ms) velocity fluctuations given by the streamwise $\langle u'u' \rangle / u_\tau^2$, wall-normal $\langle v'v' \rangle / u_\tau^2$, and spanwise $\langle w'w' \rangle / u_\tau^2$ quantities,

where $\langle \cdot \rangle$ denotes time and space averaging, the fluctuating quantities f' are calculated as $f' = f - \langle f \rangle$. In the graphs, a " + " sign denotes that the variable is normalized with u_τ , as above. For example, $uu+$ corresponds to $\langle u'u' \rangle / u_\tau^2$. For compatibility with Jimenez data at $Re_\tau = 950$, square root is taken for the streamwise, wall-normal and spanwise velocity fluctuations before comparison.

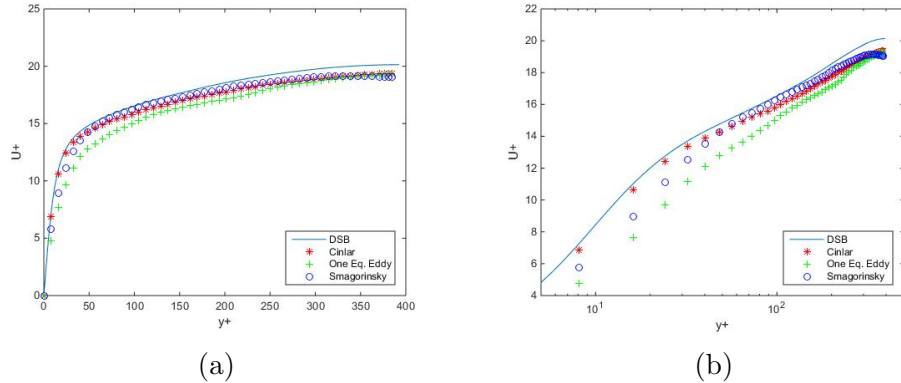


Figure 1: Channel flow comparison data for $Re_\tau = 395$, (a) mean velocity profile, (b) mean velocity profile for logarithmic scale

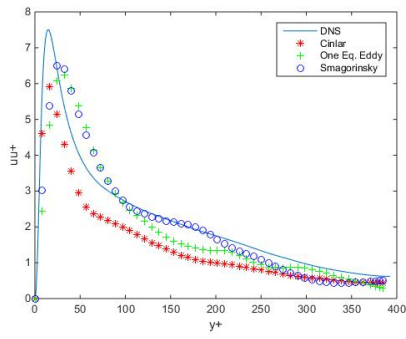
5.1. Results for $Re_\tau = 395$

In the first test case, we compare LES results with Moser DNS data for $Re_\tau = 395$ [23]. The mean streamwise velocity is given in Fig. 1, where the superscript + denotes non-dimensionalized quantities with the friction velocity u_τ . In particular, we have

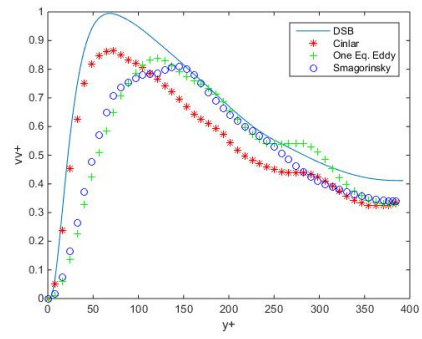
$$U+ = \langle U_1 \rangle / u_\tau, \quad y+ = yu_\tau / \nu.$$

The mean velocity profile with Çinlar SGS model is in good agreement with DNS results of Moser et.al. and LES computations of Smagorinsky and one equation eddy models. Çinlar and Smagorinsky models show the best fit regarding the mean streamwise velocity. Especially, Çinlar SGS model provides better results in the viscous wall region ($0 < y+ < 50$).

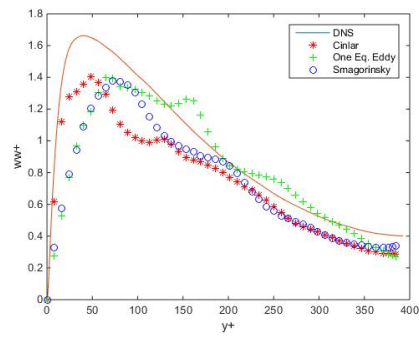
In Fig. 2, the mean square (ms) velocity fluctuations are plotted. All models predict the velocity fluctuations quite accurately. Especially in the viscous subregion, which has poor resolution for LES compared with DNS, LES results with Çinlar SGS model are remarkably good. Our model leads to over or under-prediction of the ms values from its peak to the outer layer of the channel flow where the viscosity is not prevalent. The other models also deviate from DNS, but in different regions. In particular, the value of $y+$ where ms velocities reach their peak values is best predicted by our model. Our results agree with those obtained with Smagorinsky model towards outer region, except for Fig. 2 d), where Çinlar SGS model performs better.



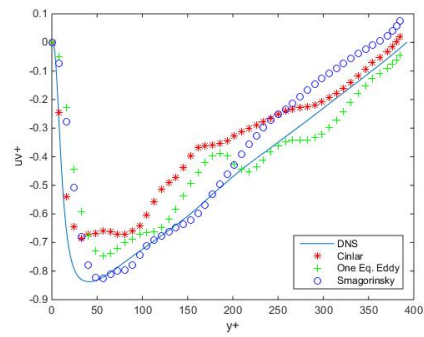
(a)



(b)



(c)



(d)

Figure 2: Channel flow comparison data for $Re_\tau = 395$, (a) ms velocity fluctuation streamwise direction; (b) ms velocity fluctuation, wall-normal direction, (c) ms velocity fluctuation spanwise direction, (d) shear stress $u'v'$ + velocity profiles

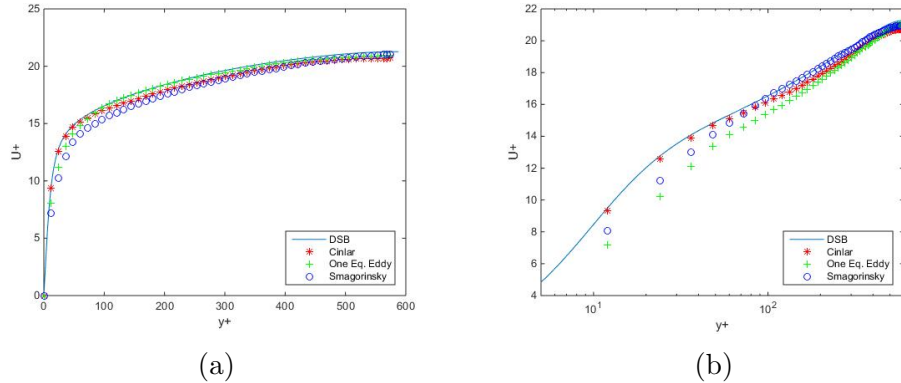


Figure 3: Channel flow comparison data for $Re_\tau = 590$, (a) mean velocity profile, (b) mean velocity profile for logarithmic scale

5.2. Results for $Re_\tau = 590$

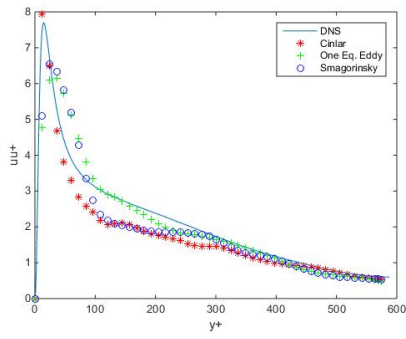
For c , mean streamwise velocity profiles are shown for DNS data and LES with the three SGS models in Fig. 3. It can be seen from the mean velocity profile graphs, Çinlar model yields the most accurate result in the viscous region. Smagorinsky model gives better approximation than one equation eddy overall, and better results towards the outer layer of the channel flow.

Fig. 4 shows comparison of ms velocity fluctuations with DNS data and LES results. LES results with Çinlar model match DNS data better than the other models in the viscous range and coincides with Smagorinsky model towards outer layer. The fluctuations in the three directions shown in Fig. 4 a)-c) attain slightly lower values than DNS data, and the shear stress is lower in magnitude as well for y^+ between 50 and 300. However, the shear stress is best approximated for $y^+ > 300$ by our model, like the viscous range. There is little discrepancy with the peak values of DNS for our model whereas the other models produce graphs which look somewhat shifted to the right.

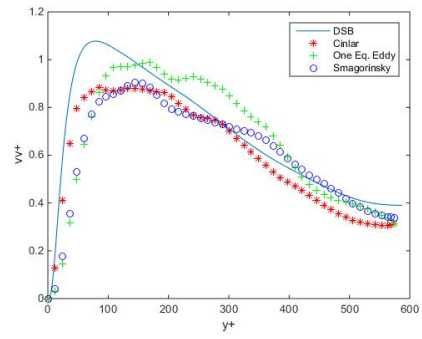
5.3. Results for $Re_\tau = 950$

The last comparison is for $Re_\tau = 950$ for validating Çinlar model. The velocity profiles are shown in Fig. 5. It can be seen that Çinlar model over-predicts the mean velocity profile throughout the channel, but with clearly less error than Smagorinsky and one equation eddy models.

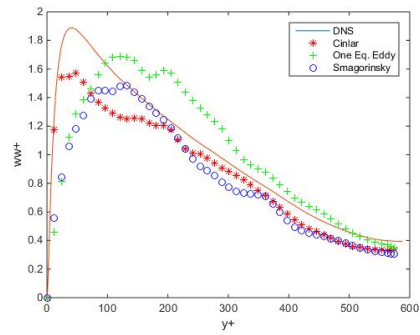
Fig. 6 presents the rms velocity fluctuations as the second-order turbulent statistics against the rms profiles from a DNS simulation of channel flow at



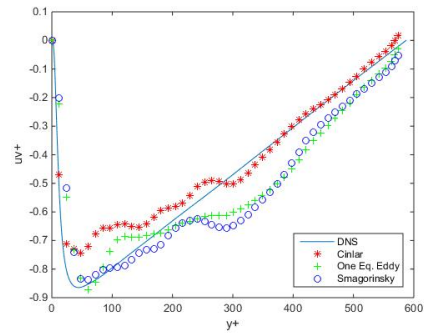
(a)



(b)



(c)



(d)

Figure 4: Channel flow comparison data for $Re_\tau = 590$, (a) ms velocity fluctuation streamwise direction; (b) ms velocity fluctuation wall-normal direction, (c) ms velocity fluctuation spanwise direction, (d) shear stress $u'v' +$ velocity profiles

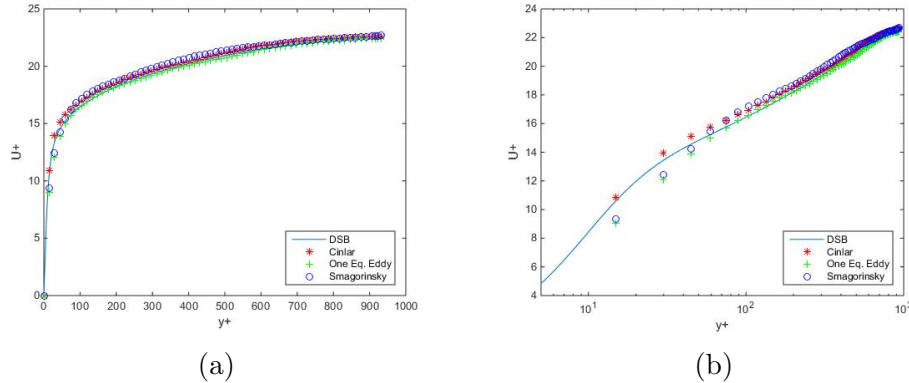


Figure 5: Channel flow comparison data for $Re_\tau = 950$, (a) mean velocity profile, (b) mean velocity profile for logarithmic scale

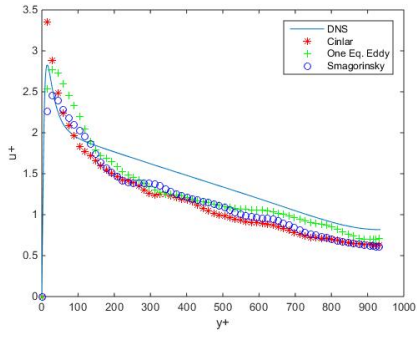
$Re_\tau = 950$ [14]. The results for the three different SGS are not significantly different from each other. All SGS models capture the general rms profile of the DNS data while Çinlar model still behaves better in the viscous range and in predicting the position of the peak values in some cases. Hence, we see that it is valid also for the high Reynolds number case.

6. Conclusion

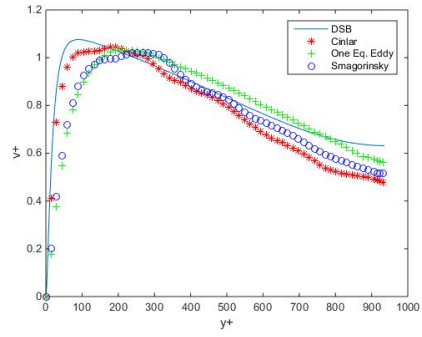
In this paper, we have modelled the Reynolds stress tensor of the generalized Çinlar random velocity field, which was shown to represent Eulerian velocity of the subscales accurately in previous work. Because an analytical expression is available for Reynolds stress, we have represented its parameters originating from the probability distributions with the resolved velocity field, in particular as functions of the resolved strain rate tensor.

Our numerical results demonstrate that LES of fully developed turbulent channel flow with Çinlar SGS model is in remarkably good agreement with the available DNS data for Reynolds numbers 395, 590 and 950, by comparison with benchmark models, namely Smagorinsky and one equation eddy. Çinlar model yields especially better results in the viscous subregion near the wall, which has poor resolution for LES compared with DNS. The computational burden is much less than one equation eddy and is observed to be as low as Smagorinsky in simulations.

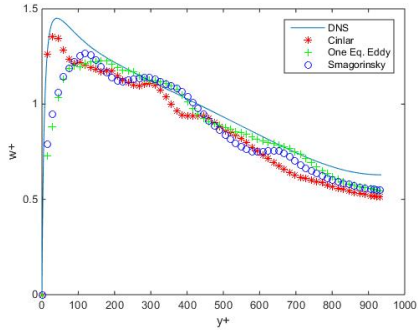
As future work, Çinlar velocity field can be extended to \mathbb{R}^3 where the



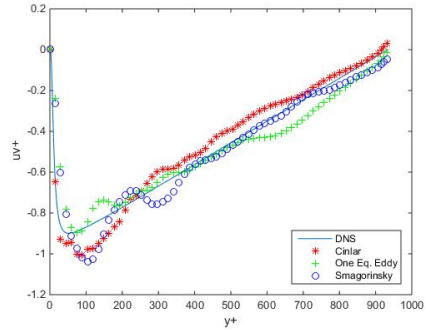
(a)



(b)



(c)



(d)

Figure 6: Channel flow comparison data for $Re_\tau = 950$, (a) rms velocity fluctuation streamwise direction; (b) rms velocity fluctuation wall-normal direction, (c) rms velocity fluctuation spanwise direction, (d) shear stress $u'v'$ + velocity profiles

basic eddy can be chosen to be the unit sphere, in analogy with the unit disk used in two dimensions, and the planar motion can be taken as a rotation.

Acknowledgements. This work was supported by The Scientific and Technological Research Council of Turkey (TUBITAK) Project No. 112T761. The numerical calculations reported in this paper were partially performed at TUBITAK ULAKBIM, High Performance and Grid Computing Center (TRUBA resources). The authors would like to thank Ayşe Gül Güngör, Alkan Kabakçioğlu, and Hasret Türkeri for their helpful discussions on the physics and simulations of the flow.

References

- [1] J. Bardina, J.H. Ferziger, W.C. Reynolds, “Improved subgrid scale models for large eddy simulation”. AIAA Pap. 80 1357 (1980).
- [2] J.M. Burgers , “A mathematical model illustrating the theory of turbulence”. Adv. Appl. Mech. **1**:171-199 (1948).
- [3] M. Çağlar, Simulation of Homogeneous and Incompressible inlar Flows. Applied Mathematical Modelling, **24**: 297-314 (2000).
- [4] M. Çağlar, Dispersion of mass by two-dimensional homogeneous and incompressible inlar flows. Applied Mathematical Modelling, **27**: 997-1011 (2003).
- [5] M. Çağlar, L. Piterbarg, T. Ozgokmen, “Parameterization of submeso-scale eddy-rich flows using a stochastic Velocity Model”. Journal of Atmospheric and Oceanic Technology **23**:1745-1758 (2006).
- [6] M. Çağlar, “Velocity fields with power-law spectra for modeling turbulent flows”. Applied Mathematical Modelling **31**:1934–1946 (2007).
- [7] E. Çinlar, “On a Random Velocity Field”, Princeton University (1993).
- [8] Clark T.L., “A small-scale dynamic model using a terrain following coordinate transformation”. J. Comput. Phys. **24**: 186–215, (1977).
- [9] J. Deardorff, “A numerical study of three-dimensional turbulent channel flow at large Reynolds numbers.”, Journal of Fluid Mechanics **41** (2): 453–480 (1970).

- [10] J. Deardorff, “Stratocumulus-capped mixed layers derived from a 3-dimensional model.” *Bound.-Layer. Meteorol.* **18** (4), 495–527, (1980).
- [11] U. Frisch, “Turbulence: The Legacy of A.N. Kolmogorov”, Cambridge University press, Cambridge (1995).
- [12] M. Germano, U. Piomelli, P. Moin, W. Cabot, ”A dynamic subgrid-scale eddy viscosity model”. *Physics of Fluids A* **3** (7): 1760–1765 (1991).
- [13] K. Horiuti, “Large eddy simulation of turbulent channel flow by one-equation modelling.” *J Phys Soc Jpn* **54**: 2855–65 (1985).
- [14] Juan C. del Alamo and Javier Jimenez, “Spectra of the very large anisotropic scales in turbulent channels”, *Phys. Fluids* **15** No. 6, pp L41-L44, (2003).
- [15] R. Kara, “Representing subgrid stress with Çinlar velocity field in large eddy simulation”, *AIP Conference Proceedings*, 1648, ICNAAM 2014, 22-28 Sep., Rhodes (2014).
- [16] R. Kara, M. Caglar, “The Energy Spectrum of Stochastic Eddies with Gamma Distribution”, *Appl. Math. Inf. Sci.* **9**, No. 1L, 39-49, (2015).
- [17] W. Kim, S. Menon, ”Application of the localized dynamic subgrid scale model to turbulent wall-bounded flows.” *AIAA Paper No. 97-0210*; (1997).
- [18] A. Leonard, ”Energy cascade in large-eddy simulations of turbulent fluid flows”. *Advances in Geophysics A* **18**:237–248 (1974).
- [19] D.K. Lilly, “On the numerical simulation of buoyant convection”. *Tellus* **14** (2):148–172 (1962).
- [20] D.K. Lilly, “The representation of small-scale turbulence in numerical simulations”., In *Proceedings of IBM scientific computing symposium on environmental sciences*, IBM form no. 320-1951. White Plains, New York, 195–209 (1967).
- [21] T.S. Lundgren, “Strained spiral vortex model for turbulent fine structure”. *Phys. Fluids* **25-12**: 2195–2203 (1982).

- [22] A. Misra, D.I. Pullin, “A vortex-based subgrid stress model for large-eddy simulation”, *Phys. Fluids* **9**: 2443–2454 (1997).
- [23] R. D. Moser, J. Kim, N. N. Mansour , “Direct numerical simulation of turbulent channel flow up to $Re = 590$.” **Phys. Fluids**, **11**(4): 943-945, (1999).
- [24] S.B. Pope, “Turbulent Flows”, Cambridge University Press, (2000).
- [25] P. Sagaut, “Large Eddy Simulation for Incompressible Flows: An Introduction”. Springer, (2005).
- [26] L.K. Shay et al., “VHF radar detects oceanic submesoscale vortex along Florida coast”. *Eos Trans.* **81**: 209–213 (2000).
- [27] U. Schumann, “Subgrid scale model for finite difference simulations of turbulent flows in plane channels and annuli.” *J Comput Phys* 18:376–404 (1975).
- [28] J. Smagorinsky, “General Circulation Experiments with the Primitive Equations”. *Monthly Weather Review* **91** (3): 99–164 (1963).
- [29] Tennekes H., Lumley J.L. “A First Course in Turbulence”. MIT, (1970).
- [30] OpenFOAM, <http://www.openfoam.com/>